Saudi Journal of Biological Sciences 28 (2021) 4461–4471

Contents lists available at ScienceDirect

Saudi Journal of Biological Sciences

journal homepage: www.sciencedirect.com

Original article

The use of biological selenium nanoparticles to suppress *Triticum aestivum* L. crown and root rot diseases induced by *Fusarium* species and improve yield under drought and heat stress

Mohamed T. El-Saadony [a,*], Ahmed M. Saad [b,*], Azhar A. Najjar [c], Seraj O. Alzahrani [d], Fatmah M. Alkhatib [e], Manal E. Shafi [c], Eman Selem [f], El-Sayed M. Desoky [g], Sarah E.E. Fouda [h], Amira M. El-Tahan [i], Mokhles A.A. Hassan [j]

[a] Department of Agricultural Microbiology, Faculty of Agriculture, Zagazig University, 44511 Zagazig, Egypt
[b] Biochemistry Department, Faculty of Agriculture, Zagazig University, Zagazig 44511, Egypt
[c] Department of Biological Sciences, Faculty of Science, King Abdulaziz University, Jeddah, Saudi Arabia
[d] Department of Chemistry, College of Science, Taibah University, P.O. Box 344, Medina, Saudi Arabia
[e] Department of Chemistry, Faculty of Applied Science, Umm Al–Qura University, Makkah, Saudi Arabia
[f] Botany and Microbiology Department, Faculty of Science, Zagazig University, Egypt
[g] Botany Department, Faculty of Agriculture, Zagazig University, 44511 Zagazig, Egypt
[h] Soil Science Department, Faculty of Agriculture, Zagazig University, 44511 Zagazig, Egypt
[i] Plant Production Department, Arid Lands Cultivation Research Institute, The City of Scientific Research and Technological Applications, SRTA-City. Borg El Arab, Alexandria, Egypt
[j] Agricultural Botany Department (Microbiology), Faculty of Agriculture, South Valley University, Qena 83523, Egypt

ARTICLE INFO

Article history:
Received 22 March 2021
Revised 15 April 2021
Accepted 18 April 2021
Available online 24 April 2021

Keywords:
Selenium nanoparticles
Antioxidant activity
Antifungal activity
Crown and root rot disease control
Fusarium spp

ABSTRACT

Fusarium species threaten wheat crops around the world and cause global losses. The global trend is toward using biological materials such as selenium (Se) in nano form to control these fungi. Bulk selenium is toxic and harmful at high doses; however, selenium nanoparticles are safe; therefore, the aim of this study to employ the biological selenium nanoparticles (BioSeNPs) synthesized by *Lactobacillus acidophilus* ML14 in controlling wheat crown and root rot diseases (CRDs) induced by *Fusarium* spp., especially *Fusarium culmorum* and *Fusarium graminearum*, and their reflection on the growth and productivity of wheat. The ability of BioSeNPs to suppress the development and propagation of *F. culmorum* and *F. graminearum* and the CRDs incidence were also investigated. The obtained BioSeNPs were spherical with a size of 46 nm and a net charge of –23.48. The BioSeNPs significantly scavenged 88 and 92% of DPPH˙ and ABTS˙ radicals and successfully inhibited the fungal growth in the range of 20–40 μg/mL; these biological activities were related to the small size of BioSeNPs and the phenolic content in their suspension. Under greenhouse conditions, the wheat supplemented with BioSeNPs (100 μg/mL) was significantly reduced the incidence of CRDs by 75% and considerably enhanced plant growth, grain quantity and quality by 5–40%. Also, photosynthetic pigments and gas exchange parameters were significantly increased as compared to chemical selenium nanoparticles (Che-SeNPs) and control. This study results could be recommended the use of BioSeNPs (100 μg/mL) in reducing CRDs incidence and severity in wheat plants, enhancing their tolerance with drought and heat stress, and increasing their growth and productivity as compared to control and Che-SeNPs.

1. Introduction

Wheat (*Triticum asetivum* L.) is a member of *Poaceae* family. It is a major cereal crop and the most important strategy crop in Egypt and worldwide. In Egypt, cereals grown on irrigated fields, wheat crop yield in season 2019–2020 was about 9.2 million tons. However, Egypt is the biggest importer of wheat globally (FAO, 2015, 2018). Wheat is a major source of energy, which contains starch

* Corresponding authors.
E-mail addresses: m_tlatelsadony@yahoo.com (M.T. El-Saadony), ahmedm4187@gmail.com (A.M. Saad).

Peer review under responsibility of King Saud University.

Production and hosting by Elsevier

https://doi.org/10.1016/j.sjbs.2021.04.043
1319-562X/

and protein. Besides, phytochemicals and dietary fibers reduce the risk of cardiovascular disease, colon-rectal cancer and type 2 diabetes; therefore it is a valuable cereal for health (Shewry and Hey, 2015).

Wheat CRDs initiated by pathogenic fungi: *Fusarium graminearum*, and *F. culmorum* and significantly affect the wheat yield worldwide. The disease severity depends on the environmental conditions of the region. The scabby grains contain mycotoxins, such as deoxynivalenol (Don), trichothecenes, zearalenone (Zon) and nivalenol (Niv) that are harmful to human and animals. These mycotoxins inhibit protein synthesis in eukaryotic cells, induce apoptosis and cause cancer (Rocha et al., 2005). The CRDs occur early in the seedling stage by fungal invading to rhizodermal root tissue and cause coleoptile infection then pathogenic fungi colonize the whole steam base, transport to vascular tissue and colonize the plant crown, all these symptoms cause crop losses (Moya-Elizondo and Jacobsen, 2016; Shah et al., 2018). Various strategies were investigated to reduce crop loss i.e., *Fusarium* resistant cultivars, chemical or biological control, and harvesting all infected crops to control CRD and *Fusarium* head blight disease of small grain cereals (Khaledi et al., 2018; Wegulo et al., 2015). Nanotechnology and nanoparticles (NPs) research have attracted a lot of interest in recent decades. There is growing attention to find effective ways for their synthesis (El-Saadony et al., 2019; El-Saadony et al., 2018; Reda et al., 2021). Microorganisms were considered bio-nano factories to provide a clean and promising alternative process for nanoparticle fabrication (Akl et al., 2020; El-Saadony et al., 2020a; Reda et al., 2020; Sheiha et al., 2020). Nanotechnology is a biofertilizer factory used in agriculture, controlling agrochemical usage, enhancing plant resistance against disease, and efficient nutrient utilization and enhanced plant growth. Recently, various studies were used nanotechnology in controlling plant disease. The nanoparticle application in various crops like wheat, corn, cucumber, and tomato enhanced crop quality and quantity. Among nanoparticles, Selenium is a valuable element for immunity and appropriate health in animals and increases plant growth. Plants are the main source of this element (Bunglavan et al., 2014; Ragavan et al., 2017). Both plants and animals have required this element at low concentrations, but it becomes toxic and harmful at higher doses. A new approach to plant fertilization is the use of selenium nanoparticles (SeNPs) as they are less toxic and their bioavailability and biological activity. Nevertheless, to produce multi-functional SeNPs, reducing agents e.g., hydrazine and sodium ascorbate, were used to chemically fabricate SeNPs. The chemical methods are expensive, require special devices, and environmentally harmful.

Therefore, scientists concern about producing green SeNPs using plant extracts and microorganisms. Green nanotechnology utilization is eco-friendly, reasonable and overcomes the use of toxic chemicals. Green selenium nanoparticles taken up by plants 20-fold faster than bulk selenium (Alagesan and Venugopal, 2019; Nandini et al., 2017). Trichogenic-selenium nanoparticles are used to control downy mildew disease in pearl millet (Nandini et al., 2017). Also, selenium nanoparticles fabricated by gamma irradiation are used to control blight disease in potatoes (El-Batal et al., 2016). In this study, SeNPs were biosynthesized by *Lactobacillus acidophilus* ML14 and characterized by TEM, FTIR, EDX, U.V., DLS, and XRD. Besides, the antioxidant and antifungal activity of Bio-SeNPs were investigated, furthermore, in vitro and in vivo study were conducted to control wheat CRD caused by *F. graminearum*, and *F. culmorum*. The fungicidal effect of Bio-SeNPs against pathogenic fungi compared to che-SeNPs and control.

Table 1
The total Phenolic and flavonoids content of BioSeNPs suspension.

Concentration (μg/mL)	TPC	TF
50	355 ± 0.9e	30 ± 0.5e
75	465 ± 1d	65 ± 0.6d
100	620 ± 1.9c	89 ± 0.8c
125	950 ± 2b	100 ± 0.8b
150	1220 ± 0.5a	120 ± 0.9a

TPC: Total phenolic content expressed as (μg GAE/mL), TF: Total flavonoids expressed as (μg QE/mL), n = 3, the data are presented mean ± SD; Mean in the same column with different lowercase letters are significantly different $p \leq 0.05$.

2. Materials

Twenty-six samples of local dairy products, including buffalo milk, cow milk, yogurt, and cheese, were collected from a private farm in Abu-Hammad city, Sharkiqa**,** Egypt. The chemicals used in this study were of analytical grade. Wheat grains (Masr1) were purchased from Filed Crop Research Institute, Agric. Res. Center (ARC). The pathogenic Fungi: *Fusarium culmorum, Fusarium graminearum F. avenaceum, F. poae, F. sporotrichioides,* and *F. cerealis* were used in this study to investigated in vitro antifungal activity of Bio-SeNPs and Che- SeNPs.

3. Methods

3.1. Isolation, screening and identification of selenium resistant bacteria

Dairy samples were homogenized in sterilized saline peptone buffer (1:9, w/v), and serial dilution was conducted to 10^7. 100 μL of each dilution was spread over the surface of selective agar media (de Man Rogosa, and Sharpe MRS agar medium) plates supplemented with different concentrations of Na_2SeO_3 (2, 4, 6, 8, and 10 mM) and incubated at 37C for 48 h. Se-resistant colonies were selected and purified then kept at 4C until use. The selected isolate was identified by morphological, biochemical and molecular tests in the Bergey manual, according to Salaj et al. (2013). The previous identification was confirmed by MALDI TOF mass spectrometry (Karaduman et al., 2017).

3.2. Production of SeNPs

3.2.1. Biosynthesis and characterization of selenium nanoparticles

Freshly cultivated isolates were inoculated into 100 ml Luria-Bertani (LB) broth and placed in a shaking incubator at 160 rpm at 35 °C until log phase of (1.5×10^8). The mixture was centrifuged at 6000 *x*g for 10 min, the bacterial pellet was obtained then homogenized in 100 ml of enrichment medium supplemented with 6.0 mM of Na_2SeO_3. The flasks were incubated under optimum conditions, and then SeNPs were harvested by centrifugation at 8000 *x*g for 10 min and washed several times with water and served to characterization (Rajasree,2015).

The Bio-SeNPs were characterized by UV–Vis spectroscopy using a spectrometer (“Laxco™, Alpha-1502 dual-beam Spectrophotometer”) according to Rajasree (2015). The morphology of nano-selenium was measured using transmission electron microscopy (TEM). Fourier transform infrared spectroscopy (FT-IR; JASCO (FTIR-6200)) was employed to explore the functional groups present in the nanoparticles. X-ray diffraction (XRD) analysis was conducted using an X-ray diffractometer (Shimadzu XRD-6000, Japan) to analyze the sample’s crystalline nature. Besides, Dynamic Light Scattering Spectroscopy (DLS) (Malvern Zetasizer Nano ZS) analyzes the selenium nanoparticles size distribution, and Zeta potential to determine the net charge at the surface of the nanoparticles.

3.2.2. Preparation of chemically produced SeNPs (Che-SeNPs)

The Che-SeNPs were produced using the wet chemical method (Boroumand et al., 2019). Briefly, drops of ascorbic acid solution (1 M) were slowly added to the Na_2SeO_3 solution (0.01 M) and stirred for 10 min. At this stage, the colorless Na_2SeO_3 gradually converted to red color, indicating the formation of che-SeNPs. The mixture was centrifuged at 7,500 × *g* for 10 min, and the pellets were obtained by rinsing several times with deionized water. The obtained che-SeNPs were lyophilized at −60 °C and stored at 4 °C.

3.3. Chemical studies

3.3.1. Total phenolics estimation

The polyphenols content of BioSeNPs suspension was estimated by the Folin-Ciocalteu method (Kalagatur et al., 2018). The results were expressed as Gallic acid equivalent (μg GAE/mL). BioSeNPs suspension (0.5 ml) was mixed with 0.5 ml of Na_2CO_3 7.5% and 0.25 ml of diluted FolinCiocalteu reagent with water (1:10, v/v), then were incubated for 30 min in the dark and the absorbance was measured at 750 nm using a microtiter plate reader (BioTek Elx808, USA).

3.3.2. Total flavonoids estimation (TFs)

The TFs of BioSeNPs suspension was evaluated by the $AlCl_3$ method (Kalagatur et al., 2018) with some modification. Briefly, 500 μL of BioSeNPs were homogenized with 70 μL of $NaNO_2$ (5%) and was incubated for five minutes at 25°C, then were mixed with 500 μL of NaOH (1 M), 150 μL of $AlCl_3$ (10%) and 1300 μL of distilled water. The previous mixture was placed in the dark for 5 min and the absorbance was measured at 430 nm using a microtiter reader (Elx808 Fisher scientific, BioTek, United States). Quercetin was used as standard and the obtained results were expressed as μg of Quercetin equivalent of BioSeNPs suspension (mL) (μg QE/mL).

3.4. Antioxidant assays

3.4.1. ABTS assay

The scavenging activity of Bio-SeNPs was estimated by Gil et al. (2002) with slight modifications. The $ABTS^+$ radical scavenging activity (%RSA) of BioSeNPs was determined by the ability of Bio-SeNPs to eliminate the $ABTS^+$ radical. One mL of BioSeNPs concentrations (50, 75, 100, 125, and 150 μg/ml) were homogenized in 3 ml of 0.1 mM ABTS and incubated for 30 min in the dark. The absorbance was evaluated at 745 nm. Tert-Butyl hydroquinone (TBHQ) was used as an antioxidant reference and ABTS reagent was control. The ABTS scavenging activity (%) of BioSeNPs was calculated from the following equation:

$$\%\text{inhibition} = \frac{\text{Abscontrol} - \text{Abssample}}{\text{Abscontrol}} \times 100$$

3.4.2. DPPH assay

The antiradical activity of BioSeNPs was processed as per Zhai et al. (2017), and Xu and Chang (2007), with a few modifications. 500 μL of BioSeNPs suspension was homogenized in 1 ml of ethanolic $DPPH^{\cdot}$ (1 mM), and placed for 30 min in the dark. The absorbance was estimated at 517 nm. The RSA % results were calculated from the following equation

$$\%DPPH\ scavenging\ activity = \frac{\text{Abs control} - \text{Abs sample}}{\text{Abs control}} \times 100$$

3.5. In-vitro antifungal activity of SeNPs against wheat Fusarium spp.

Antifungal nanoparticles activity against pathogenic fungi: *F. culmorum, F. graminearum, F. avenaceum, F. poae, F. sporotrichioides,* and *F. cerealis* were estimated by well diffusion method (Kalagatur et al., 2015). The tested fungi were spread thoroughly on the sterilized solidified PDA plates. 30 μL of each BioSeNPs and Che-SeNPs concentrations (50, 75, 100, 125, and 150 μg/ml) were loaded into wells (5 mm) that were made using sterile cork borer on PDA plate. The PDA plates were incubated for 3–5 days at 25 °C. The zone of inhibition of BioSeNPs and Che-SeNPs was measured in diameter (mm) around the wells. The MIC was estimated as the lowest concentration of BioSeNPs and Che-SeNPs that inhibit the fungal growth and MFC was the least concentration that destroys all fungal hypha. The MIC and MFC were estimated according to El-Saadony et al. (2019).

3.6. In vivo application of BioSeNPs

3.6.1. Preparation of the fungal inoculum and preparing the soil for the biological control experiment

Pots (25 cm in diameter) were sterilized by formalin solution (5%) for 15 min and then were left several days to get rid of the formalin poisonous effect. Soil (50% sand and 50% clay) was autoclaved at 121 ℃ for two hours and left for two weeks before cultivation. The inoculum was prepared by inoculating pieces of *F. culmorum, F. graminearum, F. avenaceum, F. poae, F. sporotrichioides,* and *F. cerealis* PDA plates in 500 ml conical flasks containing 200 g of autoclaved wheat grains and were incubated at 27C for 21 days. Sterilized pots were filled with autoclaved soil (6.6 Kg) and were infected with the tested *Fusarium* inoculum. The inoculum was mixed with the soil at the rate of 5% of soil weight (v/w). The infected soil was watered and left for ten days before seeding to stimulate the fungal growth and ensure its dispersal in the soil. The non-infected soil was inoculated with the fungal-free wheat grain medium at the same rate (Janga et al., 2017).

3.6.2. In vivo study (under greenhouse conditions)

Healthy wheat grains cv. Masr1 were sterilized in 1% NaOCl (Sodium hypochlorite) for 2 min and then rinsed three times in sterile water to eliminate surface seed secondary fungal pathogens blot-dried to remove excess water as mentioned by Parsons and Munkvold (2012). The wheat grains cv. Masr-1 were soaked in 50 ml suspension of each BioSeNPs (50, 75, and 100 μg/mL), Che-SeNPs (50, 75, and 100 μg/mL) for 24 h (Ma et al., 2008). For control treatments, grains were soaked individually in 50 ml of sterile water for 24 h, according to Xue et al. (2017). Treated grains were air-dried and five grains were planted per pot (25 cm) containing infected or non-infected soils. Water-soaked seeds were sown in infested and non-infested soil to serve as a positive and negative control, respectively. Three pots were used for each particular treatment. All pots were watered every 15 days with bioagent water. Disease parameter was recorded as disease incidence (%) of pre, post-emergence, damping-off and healthy survival after three months.

The disease severity index (DSI) was calculated using the scale values

$$DSI = \frac{\varepsilon nx}{NX} \times 100$$

($\sum$ (n, number of plants in a disease scale category × disease scale category)/ (N, the total number of plants X, maximum disease scale category)) × 100) according to Chekali et al. (2011).

3.6.3. Growth and yield attributes

Growth parameters including fresh, dry weights (gram) and plant height (cm) were estimated. The root system was tapped out of the pot and was gently washed by tap water, for obtaining fresh and dry weight, the roots were blot-dried to remove excess water then the fresh weight (FW) was recorded. Shoots and roots

were dried in an oven under 65 °C for several days until constant weight to obtain dry weight (DM). Spike length (cm), spike number and weight of the 1000 grains (g) were calculated.

3.6.4. Photosynthetic pigments and gas exchange assessments

Total chlorophyll and carotenoids were estimated as per Nagata and Yamashita (1992), gas exchange parameters (net photosynthetic, transpiration, and stomata conductance g_s) were evaluated according to Drake et al. (2013) in wheat leaves.

3.7. Statistical analysis

The obtained data were statistically analyzed by ANOVA test at $P \leq 0.05$, which was performed with IBM SPSS v20.0. All values are means (n = 5, except n = 30 for yield components), the replicate means were compared by LSD test.

4. Results

4.1. Isolation and identification of Lactobacillus (lactic acid bacteria)

Forty isolates were obtained from different dairy samples on MRS plates and coded as (ML1, ML2,. . .ML40), 15 isolates appeared at MRS plates supplemented with sodium selenite (2 mM), 7 isolates occurred at 4 mM concentration, and one isolate was survived at 6 mM concentration and it was served for identification resistant to Na2SeO3 (6 mM) was identified by a light microscope, tA light microscope, t, and identified the optimum isolate resistant to Na2SeO3 (6 mM). The obtained pure isolate after the screening was a long rod, Gram-positive, non-spore-forming and motile. The obtained results revealed that this bacterium similar to the *Lactobacillus* species based on the morphologically, physiologically and biochemically tests carried out as per Bergey's Manual Salaj et al. (2013), and identified as *Lactobacillus acidophilus* ML14, further identification was conducted by MALDI TOF Mass spectrometry. The attained result showed 98% of our isolates to Lactobacillus spp. Based on MALDI-TOF score, the local bacterial isolate, *Lactobacillus acidophilus* ML14 is similar to *Lactobacillus acidophilus* DSM 20,242 DSM.

4.2. Characterization of selenium nanoparticles produced by Lactobacillus acidophilus ML14

Bio-SeNPs were primarily characterized by U.V. spectrophotometer. The absorbance was increased with increasing incubation time. The SeNPs suspension was showed a sharp Plasmon peak at 300 nm (Fig. 1**A**).

Size and morphology of SeNPs were identified by TEM. Fig. 1B showed TEM image and histogram of BioSeNPs, the image exhibited a spherical shape with an average diameter between 65 and 88 nm.

The crystallite nature of Bio-SeNPs was examined by XRD; this analysis determined crystallite materials and provided details about unit cell dimensions. Fig. 1**C** showed that BioSeNPs were highly crystalline and all diffraction peaks have been well indexed as 28.37°, 30.89°, 40.31°, 44.92°, 55.88°, 65.94°, 74.89° and 83.38°, which correspond to 100, 101, 110, 102, 201, 210, 112 and 202 crystal planes, respectively.

FTIR spectroscopy is useful in acquiring the chemical composition of active compounds on the Bio-SeNPs surface as capping agents on the nanoparticles obtained by *Lactobacillus acidophilus* ML14 supernatant. These compounds are responsible for stabilizing the Bio-SeNPs. The results showed twelve distinct peaks between 3435.27 and 544.04 cm^{-1} (Fig. 1**D**). The spectrum of SeNPs has vibrational and stretching functions at wavelengths of 1407.78, 1265.05, 1128.84 and 1068.11 cm^{-1} corresponding to C–H, C = C, O–H and C–O, respectively. The band at 2446.14 cm^{-1} for the C–H stretch of aryl acid. The strong band found at 1638.89 cm–1 was characteristic of C = C stretch of an aromatic ring, N–H bending of amine and a C = O stretch of polyphenols. 3435.27 cm^{-1} indicates O–H groups in water and alcohol. The peaks at 994.25, 951.81, 8278.35, and 609.52 cm^{-1} are due to aromatic C–H bending. The peak at 544.04 cm^{-1} indicates metal–carbon stretch. Peaks that observed between 1100 and 1000 can indicate the C–O group.

The DLS analysis characterized the size and charge of Bio-SeNPs, the size of the obtained BioSeNPs was about 46 nm (Fig. 1**E**), with PDI value of 0.04, and Zeta potential value of SeNPs was (–23.48 mV) (Fig. 1**F**).

4.3. Chemical studies

4.3.1. Antioxidant activity, phenolic, and flavonoids content of Bio-SeNPs

Fig. 2 showed the antiradical activity of Bio-SeNPs suspension produced by *Lactobacillus acidophilus* ML14. Bio-SeNPs suspension (150 μg/mL) was significantly $p \leq 0.05$ scavenged 88 and 92% of $DPPH^{\cdot}$ and $ABTS^{+}$ radicals compared to TBHQ. The phenolic and flavonoids content in BioSeNPs were 1220 and 120 μg/mL, respectively (Table 1).

4.3.2. In-vitro antifungal activity of CheSeNPs and BioSeNPs against wheat pathogenic fungi

Table 2 showed the inhibition zones diameters of Che-SeNPs and BioSeNPs against pathogenic fungi. Generally, BioSeNPs concentrations more effective than Che-SeNPs against tested fungi. The IDZs were in the range of 12–30 mm (Che-SeNPs) and were ranged from 18 to 33 mm (BioSeNPs). *F. cerealis* and *F. sporotrichioides* were more sensitive fungi to Che-SeNPs and BioSeNPs concentrations, however, *F. graminearum* and *F. culmorum* were the most resistant to SeNPs, therefore these two fungi used in *in vivo* experiment. Also, Table 2, the MIC and MFC of Che-SeNPs and BioSeNPs, the MIC and MFC of Che-SeNPs significantly increased with 15% about BioSeNPs and that indicate the activity of BioSeNPs

The Che-SeNPs were significantly reduced the fungal growth in the MIC range (25–45 μg/mL). However, BioSeNPs have successfully inhibited the tested fungi in the MIC range of 20–40 μg/mL. Fig. 3 showed the interaction between BioSeNPs concentrations and *Fusarium culmorum*, and it was observed that the fungal mycelia were destroyed.

4.4. In vivo control of wheat CRDs under greenhouse conditions

4.4.1. Disease parameters

The results in Table 3 are in harmony with in vitro antifungal results in Table 2. The Bio-SeNPs (100 μg/mL) showed the highest percentage of healthy survival plants (81%) followed by Che-SeNPs, i.e., 75%, with a relative increase of about 91 and 81%, respectively, as compared to control. There were significant differences between the reduction effect of Che-SeNPs and BioSeNPs on pre-emergence damping-off whereas, Bio-SeNPs (100 μg/mL) significantly $p \leq 0.05$ reduced pre-emergence with about 60 and 87% against both pathogenic fungi with a relative increase 55% as compared to control and 18% over Che-SeNPs, besides, Bio-SeNPs (100 μg/mL) banned post-emergence of disease. Bio-SeNPs (100 μg/mL) significantly $p \leq 0.05$ reduced the incidence and severity of wheat CRD by 73, 88%, respectively (Fig. 4).

4.4.2. Growth parameters

As a result of reducing disease incidence and severity by Bio-SeNPs (100 μg/mL), a significant increase in all plant growth is

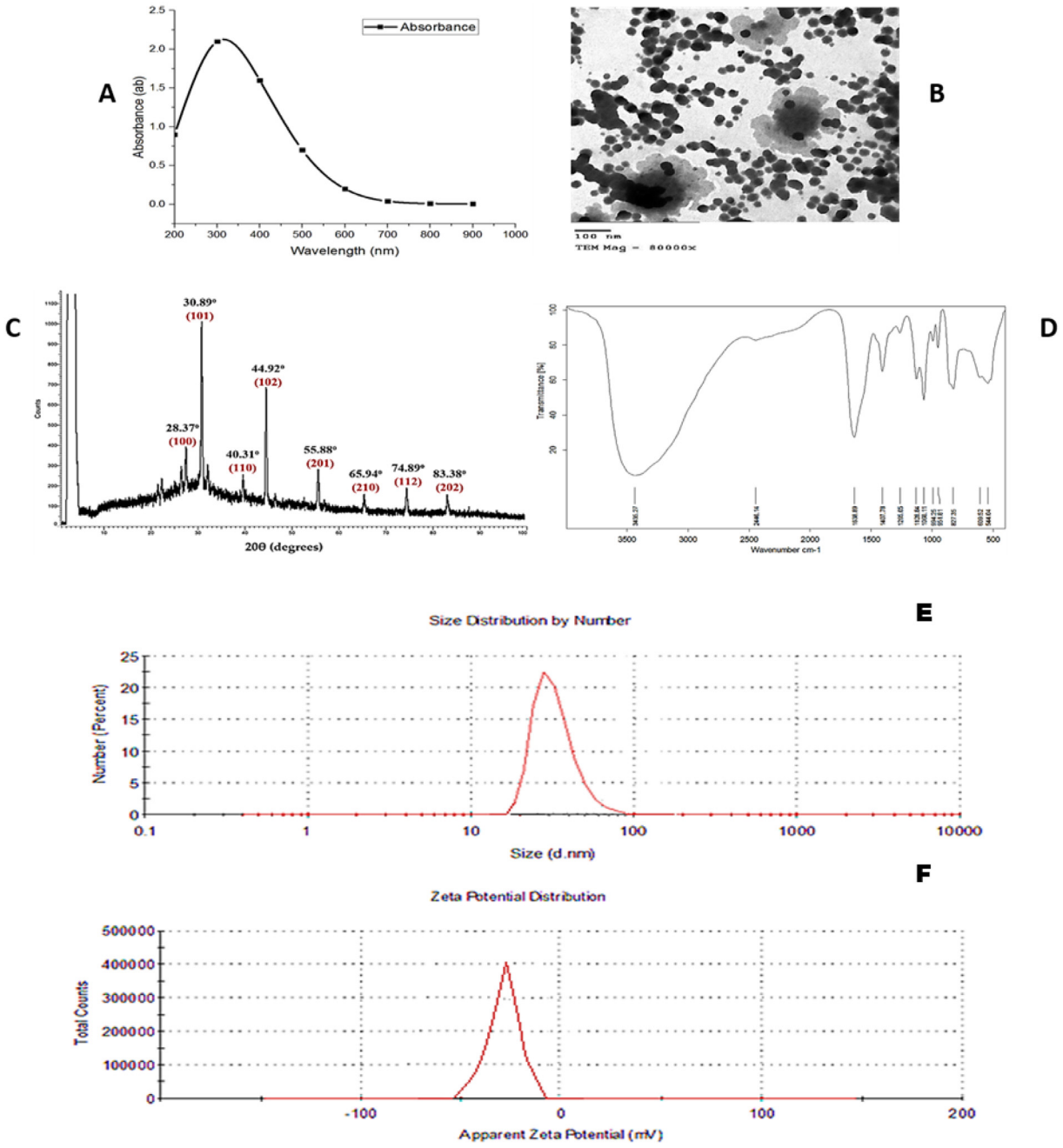

Fig. 1. Characterization of Bio-SeNPs produced by *Lactobacillus acidophilus* ML14 filtrate. (**a**) UV– Visible spectrum showing the absorption peak at 300 nm. (**b**) Transmission electron microscopic (TEM) view of Bio-SeNPs. (**c**) XRD spectrum showing the presence of Bio-SeNPs. (**d**) FTIR spectrum showing active groups in nanoparticles suspension (**E**) the size of BioSeNPs (**F**) net charge at BioSeNPs surface.

shown in Table 4 and Fig. 4. The Bio-SeNPs (100 μg/mL) significantly increased spike, root and shoot's the length and weight, grain quantity in spike, and 1000 grain weight by 5–40% compared to control with a relative increase of about 20% over Che-SeNPs (100 μg/mL).

4.5. Photosynthetic pigments and gas exchange

Wheat samples treated with Bio-SeNPs (100 μg/mL) showed higher contents of total carotenoids and chlorophyll Table 5. The total carotenoids and chlorophyll content in wheat treated with Bio-SeNPs (100 μg/mL) significantly increased with 12–32% over control. Also, Table 5 showed the gas exchange parameters, i.e., transpiration (Tr), net photosynthesis (Pn), and the conductance of stomata (g_s). The addition of Bio-SeNPs (100 μg/mL) to wheat samples significantly increased these parameters as compared to CheSeNPs and control.

5. Discussion

Use of biological mass such as bacteria, fungi, yeast, plant extract or plant biomass, and algae extract, or biomass could be an alternative to these methods for the synthesis of nanoparticles in an eco-friendly manner, safely, less time consuming, and low cost (El-Saadony et al., 2021a). Powerful antioxidant and antifungal activity of obtained BioSeNPs attributable to reducing CRD inci-

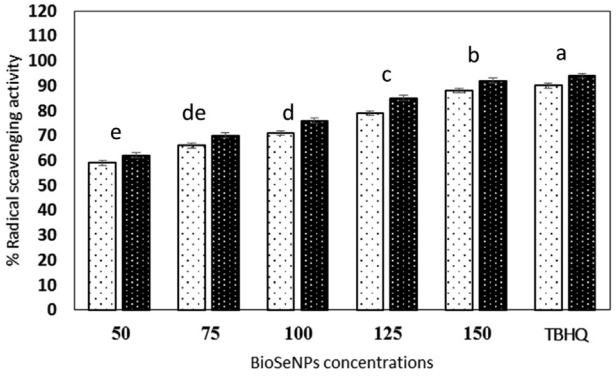

Fig. 2. Radical scavenging activity of Bio-SeNPs against DPPH, $ABTS^{+}$ radicals after 30 min, data are presented mean ± SE, the means with different lowercase letters indicate significant differences $p \leq 0.05$.

dence and counteracting drought and heat stress in wheat plant. In this study, SeNPs were synthesized by *Lactobacillus acidophilus* ML14; several bacteria were screened for their ability to synthesis Intra/extracellular SeNPs of uniform size and shape. The physico-chemical properties of SeNPs may fluctuate according to the organism type uses in the production process (Ahmed et al., 2013; Srivastava and Mukhopadhyay, 2015).

Various advanced analytical instruments characterized the Bio-SeNPs and they were monodispere. Spherical crystalline and that following the previous studies, UV–Vis spectrum is the most basic and important technique for identifying and characterizing nanoparticles. Various studies stated that SeNPs production methods affect the absorbance peaks in UV–Vis spectra. SeNPs obtained by *Klebsiella pneumonia* showed absorbance peaks between 200 and 300 nm with strong absorbance at 265 nm (Fesharaki et al., 2010). Zhang et al. (2011) and Hariharan et al. (2012) found that SeNPs produced by *Saccharomyces cerevisiae*, and *Pseudomonas alcaliphila* showed absorption peaks at 200 and 300 nm, respectively and that indicate the presence of SeNPs. On the other hand, Hu et al. (2012) presented comparable results to ours where selenium nanoparticles size was in the range of 20–80 nm. Also, Chen et al. (2008) synthesized spherically shaped and 44–92 nm-sized SeNPs by *Undaria pinnatifida* extract. Furthermore, the size of SeNPs fabricated by *Klebsiella pneumoniae* was 245 nm (Fesharaki et al., 2010). The size ranged 50–400 nm spherical SeNPs produced by *S. leopoliensis* (Hnain et al., 2013), *L. acidophilus* produced 50–500 nm SeNPs, *Bifidobacterium* sp. produced 400–500 nm SeNPs and *K. pneumoniae* produced 200–300 nm SeNPs (Sasidharan et al., 2014). The produced SeNPs were monodisperse because the less PDI value (Bihari et al., 2008) and net negative charge on their surface prevented the aggregation of nanoparticles in the suspension and achieved stability and may keep more than a month (Dhanjal and Cameotra, 2010). Besides, they were crystalline based on diffraction peaks of X-ray according to Ingole et al. (2010); Dorofeev et al. (2012); Srivastava and Mukhopadhyay (2013).

The BioSeNPs exhibited considerable antioxidant activity (Gunti et al., 2019; Kapur et al., 2017; Shubharani et al., 2019; Vyas and Rana, 2017), because of the occurrence of phenolic compounds and flavonoids content in the nanoparticles suspension besides, their small size (Huang et al., 2007), these active compounds are derived from the rich bacterial media especially yeast extract in LB media (El-Saadony et al., 2021b; Vieira et al., 2016). The scavenging activity significantly increased in the concentration-dependent matter (Shubharani et al., 2019). Uddin et al. (2012) showed that SeNPs produced by Leaves Extract of *Withania somnifera* contain active phytochemicals that might be combined with the metal solution to give the nanoparticles, the phenolic

Table 2
In vitro antifungal activity of chemical and biological selenium nanoparticles against wheat pathogenic fungi expressed as inhibition zones diameters (mm).

Fungi	Concentration (μg/mL) /Inhibition zones (mm)												Che-SeNPs		BioSeNPs	
	Chemical Se nanoparticles					Biological Se nanoparticles										
	50	75	100	125	150	50	75	100	125	150	MIC	MFC	MIC	MFC
F. graminearum	15 ± 0.6bF	18 ± 0.2bcE	21 ± 0.2bcD	23 ± 0.4cC	27 ± 0.5cAB	17 ± 0.2bcEF	21 ± 0.2bcD	23 ± 0.1cC	25 ± 0.2 dB	29 ± 0.3cA	40b	75b	35b	65b
F. cerealis	17 ± 0.2aF	20 ± 0.1abE	24 ± 0.8aD	27 ± 0.2abC	30 ± 0.5aB	20 ± 0.2aE	24 ± 0.3aD	27 ± 0.2aC	31 ± 0.2aAB	33 ± 0.4aA	25e	50e	20e	40e
F. poae	16 ± 0.5abF	18 ± 0.5bcEF	22 ± 0.2bD	27 ± 0.6abC	30 ± 0.1aB	19 ± 0.2abE	22 ± 0.2bD	26 ± 0.5abCD	29 ± 0.3bBC	32 ± 0.2abA	30d	60d	25d	45d
F. avenaceum	15 ± 0.7bG	19 ± 0.6bF	23 ± 0.4abE	26 ± 0.8bC	29 ± 0.1bB	18 ± 0.2bFG	21 ± 0.3bcEF	24 ± 0.3bD	28 ± 0.2cBC	31 ± 0.5bA	35c	65c	30c	55c
F. culmorum	12 ± 0.1cG	15 ± 0.7cF	19 ± 0.1cE	22 ± 0.8dD	26 ± 0.4 dB	15 ± 0.5cF	18 ± 0.4cEF	22 ± 0.2dD	24 ± 0.4deC	28 ± 0.5dA	45a	80a	40a	70a
F. sporotrichioides	17 ± 0.4aF	21 ± 0.9aD	24 ± 0.3aC	28 ± 0.6aB	30 ± 0.3aA	19 ± 0.2abE	23 ± 0.2abCD	27 ± 0.3aBC	30 ± 0.1abA	32 ± 0.5abA	25e	50	20e	45d

Mean ± SD; n = 3; Means in the same column with different lowercase letters are significantly different, different uppercase letters in the same raw indicate significant difference between chemical and biological selenium nanoparticles against tested fungi $p \leq 0.05$

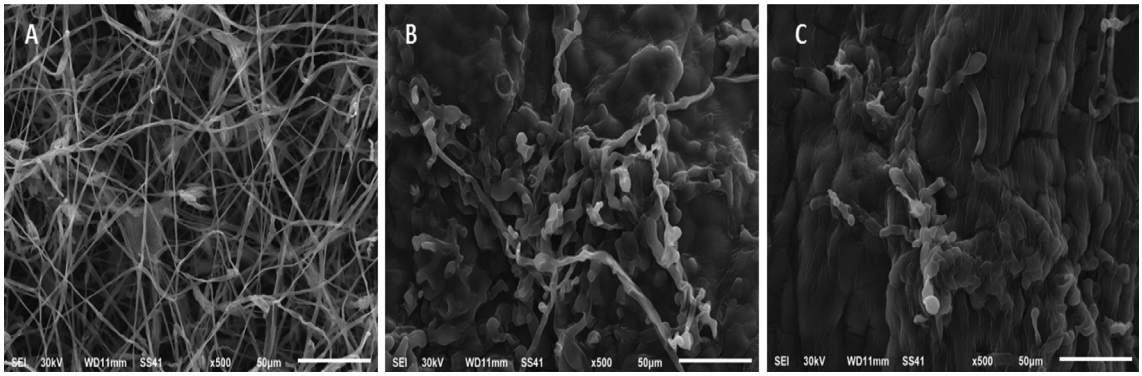

Fig. 3. Scanning electron microscope (SEM) of (A) *Fusarium culmorum* control (B) the effect of Che-SeNPs (100 μg/mL) on *F. culmorum* growth, (C) the effect of BioSeNPs (100 μg/mL) on *F. culmorum* growth.

Table 3
In vivo effect of Che-SeNPs and BioSeNPs treatments at concentrations (50, 75, and 100 μg/mL) on Masr1 wheat cultivar CRDs.

Treatment	Disease parameter					
	Pre (%)	Post (%)	CRD (%)	Healthy (%)	Disease incidence (%)	Disease severity(%)
Control	0	0	0	100aE	0	0
Fusarium culmorum	28.5aA	32aA	45aA	0	90aA	85aA
Fusarium graminearum	19bA	8b	21b	7bE	81bA	67bA
CheSeNPs 50 (control)	0	0	0	100aE	0	0
CheSeNPs 50 + *F. culmorum*	23aB	11cB	32abB	30bcE	70aB	50.3aB
CheSeNPs 50 + *F.graminearum*	13bB	0	19bB	33bE	66bB	41.33bB
BioSeNPs 50 (control)	0	0	0	100aD	0	0
BioSeNPs 50 + *F. culmorum*	20.8	8.5	25	45bcD	58aC	35a
BioSeNPs 50 + *F.graminearum*	9.9	0	16.4	51bD	40bC	26b
CheSeNPs 75 (control)	0	0	0	100aC	0	0
CheSeNPs 75 + *F. culmorum*	18.3aC	4.5aC	22aC	58.63cC	39aD	16.9aD
CheSeNPs 75 + *F.graminearum*	6.1bC	0	15bC	72.33bC	27.8bD	14.32abD
BioSeNPs 75 (control)	0	0	0	100aBC	0	0
BioSeNPs 75 + *F. culmorum*	16.6aD	3.5aD	20aD	60cBC	36aC	15.5aC
BioSeNPs 75 + *F.graminearum*	5.9bD	0	13.33bD	73.33bBC	20bC	13.3bC
CheSeNPs 100 (control)	0	0	0	100aB	0	0
CheSeNPs 100 + *F. culmorum*	15aDE	0.9aE	15aE	70bcB	30aE	10.5aE
CheSeNP 100 + *F.graminearum*	5.1bDE	0	9bE	75bB	25bE	8.9abE
BioSeNPs 100 (control)	0	0	0	100aA	0	0
BioSeNPs 100 + *F. culmorum*	12.3aE	0	13aF	78.33cA	24.9aF	9.5aF
BioSeNPs100 + *F.graminearum*	2.3bE	0	6bF	81bA	19bF	8abF

Mean in the same column with different lowercase letters are significantly different within treatment $p \leq 0.05$, different uppercase letters indicate significant difference between groups, n = 30; CRD: crown and root rot disease.

compounds capped the surface of SeNPs and encouraged their stability. The antioxidant potential of SeNPs due to the electron-donating ability of bioactive compounds on the nanoparticles surface. Also, our BioSeNPs presented a strong antifungal activity following Gunti et al. (2019) and Pierard et al. (1997), who used the SeNPs produced by *Emblica officinals* as anti-dandruff shampoo to treat fungal infections, also, Shahverdi et al. (2010) found that SeNPs fabricated by *K. pneumonia* reduced the fungal growth in the range of 10–260 μg/mL against *Malassezia sympodialis, Aspergillus terreus*, and *Malassezia furfur*. Furthermore, Kazempour et al. (2013) found that the SeNPs with MIC levels 250, 2000 μg/mL inhibited the *Aspergillus brasiliensis,* and *Candida albicans* growth, respectively. The antimicrobial mechanism of nanoparticles was briefed by DNA damage and cell wall disruption. Nanoparticles electrostatically interact with the cell wall or cell membrane, causing the cell wall disruption. Therefore, large molecules pass through the cell membrane and destroy DNA, which causes cell death (Anyasi et al., 2017; Dakal et al., 2016; El-Saadony et al., 2020b; Kaur, 2011). Also, Shenashen et al. (2017) reported that nanoparticles disturbed the fungal cell membrane and leakage in fungal cells, which cause hypha malformation and cell death.

The application of nano-metals in plant disease management is promising as an alternative to chemical pesticides. DNA-directed AgNPs grown on graphine oxide (Go) suppresses bacterial spot of tomato caused by *Xanthomonas perforins* (Ocsoy et al., 2013) and powdery mildew in cucurbits when applied as a foliar spray at 100 ppm concentration (Lamsa et al., 2011). Furthermore, Jo et al. (2009) evaluated the antifungal activity of silver ions and silver nanoparticles foliar against, *Bipolaris sorokiniana* and *Magnaporthe grisea* and they found a reduction of fungal growth and disease incidence in ray grass, the higher surface area to volume of metal nanoparticles may the reason of biological activity (Shah and Belozerova, 2009). Also, the utilization of these nanoparticles enhances the antioxidant potential of treated plants under their ability to participate in cellular redox reactions since SeNPs were significantly increased the antioxidant enzymes, phenolic compounds, and amino acids in tomato leaves (Hernández-Hernández et al., 2019). Also, the additional promoting effect of SeNPs (1 ppm) produced by gamma irradiation inhibited lipid peroxidation. It decreased MDA concentration in ryegrass (*Lolium perenne*) as reported by Hartikainen et al. (2000). Likewise, Ismail et al. (2016) and Zakharova et al. (2017) evaluated the syndicate effect

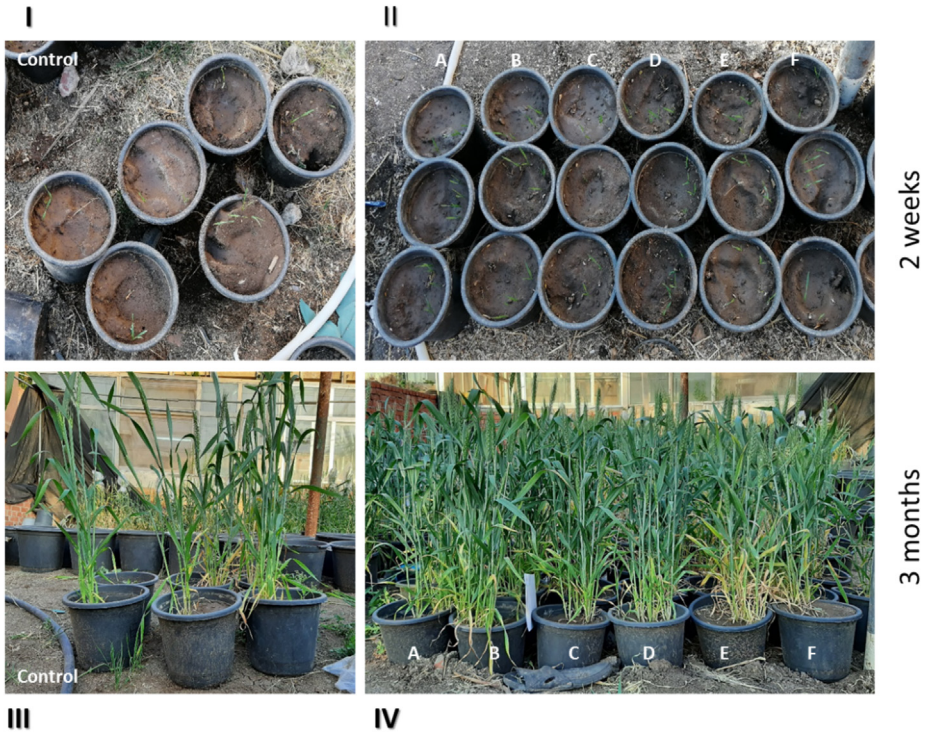

Fig. 4. *In vivo* experiment control of CRDs in infected wheat with *Fusarium* under greenhouse conditions**:** 2 weeks aged wheat control (I), 2 weeks aged SeNPs-supplmented wheat (II), 3 month aged wheat control (III), 3 month aged SeNPs-supplmented wheat (IV). (A-C) wheat treated with BioSeNPs concentrations (50, 75, and 100 μg/mL), (D-F) wheat treated with CheSeNPs concentrations (50, 75, and 100 μg/mL).

Table 4
In vivo effect of Che-SeNPs and BioSeNPs treatments at concentrations (50, 75, and 100 μg/mL) on plant growth parameters in Masr1 wheat cultivar.

Treatment	Plant growth parameters									
	1	2	3	4	5	6	7	8	9	10
Control	3.4aG	2.1a	19a	8.1a	16.9a	79a	3aB	10.6a	47a	43a
Fusarium culmorum	2.9b	1.5c	14c	3.1c	12.3c	68c	2b	9.9b	44b	37b
Fusarium graminearum	3.1ab	1.7b	16b	5.1b	14b	75b	3a	8.9c	41c	25c
CheSeNPs 50 (control)	3.6aF	2.3a	19.4a	8.39a	17.2a	79.5a	3aB	10.9a	50a	45a
CheSeNPs 50 + *F. culmorum*	3.0c	1.7c	15.1c	4.2c	13.5c	69c	2b	10ab	46b	40b
CheSeNPs 50 + *F.graminearum*	3.3b	1.9b	16.8b	6.1b	15b	71b	3a	9.5b	43c	39bc
BioSeNPs 50 (control)	3.7aE	2.4a	19.5a	8.52a	17.5a	80.2a	3a	11.1a	52a	46.9a
BioSeNPs 50 + *F. culmorum*	3.1bc	1.75c	15.3c	4.34c	13.9c	69.8c	2b	10.6b	48b	44b
BioSeNPs 50 + *F.graminearum*	3.2b	1.95b	17b	6.18b	15.1b	73b	3a	9.8c	44.5c	40c
CheSeNPs 75 (control)	3.8aD	2.49a	19.6a	8.6a	17.6a	80.6a	3aA	11.3a	54a	49a
CheSeNPs 75 + *F. culmorum*	3.1c	1.7c	15.4c	4.5c	14.2c	71c	3a	10.8b	49b	46b
CheSeNPs 75 + *F.graminearum*	3.5b	2.1b	17.1b	6.2b	15.23b	74b	3a	10bc	46c	41c
BioSeNPs 75 (control)	3.9aC	2.55a	19.8a	8.9a	17.9a	80.8a	3aA	11.4a	55a	50a
BioSeNPs 75 + *F. culmorum*	3.1c	1.7c	14.9c	4c	12.3c	71c	3a	10.9b	50b	47b
BioSeNPs 75 + *F.graminearum*	3.5b	2.1b	17b	6.1b	15b	75b	3a	10.2c	48c	42c
CheSeNPs 100 (control)	4.2aB	2.75a	20.8a	9.9a	18a	81a	3aA	11.5a	56a	51a
CheSeNPs 100 + *F. culmorum*	3.6c	2.2c	15c	4.1c	13c	72c	3a	11ab	51b	47b
CheSeNPs 100 + *F.graminearum*	3.9b	2.5b	18b	7.1b	16b	76b	3a	10.8b	49bc	45bc
BioSeNPs 100 (control)	4.5aA	3.1a	21.6a	10.7a	18.5a	82a	3aA	12a	58a	52a
BioSeNPs 100 + *F. culmorum*	3.9bc	2.5bc	16.5c	5.6c	13.9c	73c	3a	11.4b	56b	50b
BioSeNPs100 + *F.graminearum*	4.1b	2.7b	18.8b	7.9b	16b	77b	3a	11bc	50c	48c

Mean in the same column with different lowercase letters are significantly different in one group $p \leq 0.05$. Different upper letters are different between groups; n = 30. Plant growth parameters; 1: Root fresh weight (g), 2: Root dry weight (g), 3: Shoot fresh weight (g), 4: Shoot dry weight (g), 5: Root length (cm), 6: Shoot length (cm), 7: Tiller (No), 8: Spike length (cm), 9: Grains number (No), 10: 1000 grains weight (g).

of silver and selenium nanoparticles against *A. solani* that initially cause blight disease of potato. No available studies on the use of SeNPs synthesized by bacteria to control plant disease management.

On the side of plant growth and productivity, several studies reported that SeNPs increased quality parameters and yield of many crops i.e. pumpkins (*Cucurbita pepo*), potato, soybean and Canola (*Brassica napus* L.) at a low concentration (Djanaguiraman et al., 2005; Germ et al., 2005; Lyons et al., 2009), cluster bean (*Cyamopsis tetragonoloba* L.) (Ragavan et al., 2017). On the same route, Hernández-Hernández et al. (2019) found that tomato yield was increased by up to 21% with 10 mg L^{-1} of SeNPs. Also, Ikram et al. (2020) found that the usage of SeNPs 30 mg/L as foliar at wheat remarkably increased plant height, shoot length, shoot fresh

Table 5
In vivo effect of Che-SeNPs and BioSeNPs treatments at concentrations (50, 75, and 100 μg/mL) on Gas exchange parameters in Masr1 wheat cultivar.

Treatment	Gas exchange parameters				
	Total chlorophyll	Total carotenoids	Net photosynthetic	Transpiration	conductance of stomata (g_s)
Control	2.06a	0.76a	11.08a	7.28a	0.41aG
Fusarium culmorum	1.54c	0.58c	6.40c	2.60c	0.23c
Fusarium graminearum	1.67b	0.60b	7.04b	3.24b	0.25c
CheSeNPs 50 (control)	2.41a	0.79a	11.23a	7.43a	0.44aF
CheSeNPs 50 + *F. culmorum*	1.58c	0.60c	9.57c	5.77c	0.32bc
CheSeNPs 50 + *F.graminearum*	2.27b	0.68b	9.83b	6.03b	0.33b
BioSeNPs 50 (control)	2.42a	0.8a	11.4a	7.6a	0.45aE
BioSeNPs 50 + *F. culmorum*	1.61c	0.61c	8.5c	4.9c	0.3bc
BioSeNPs 50 + *F.graminearum*	2.30b	0.68b	9.9b	6.4b	0.33b
CheSeNPs 75 (control)	2.43a	0.81a	11.76a	7.96a	0.46aD
CheSeNPs 75 + *F. culmorum*	1.67c	0.62c	7.83c	4.03c	0.27c
CheSeNPs 75 + *F.graminearum*	2.30b	0.69b	10.15b	6.35b	0.34b
BioSeNPs 75 (control)	2.47a	0.83a	12.18a	8.38a	0.48aC
BioSeNPs 75 + *F. culmorum*	1.82c	0.63c	8.23c	4.43c	0.28c
BioSeNPs 75 + *F.graminearum*	2.33b	0.71b	10.31b	6.51b	0.36b
CheSeNPs 100 (control)	2.50a	0.86a	12.41a	8.61a	0.51aB
CheSeNPs 100 + *F. culmorum*	1.97c	0.65c	8.79c	4.99c	0.30c
CheSeNPs 100 + *F.graminearum*	2.35b	0.73b	10.72b	6.92b	0.38b
BioSeNPs 100 (control)	2.53a	0.89a	12.66a	8.86a	0.54aA
BioSeNPs 100 + *F. culmorum*	2.13c	0.66c	9.06c	5.26c	0.31c
BioSeNPs100 + *F.graminearum*	2.37b	0.74b	10.99b	7.19b	0.39b

Mean in the same column with different lowercase letters are significantly different in one group $p \leq 0.05$. Different upper letters are different between groups; n = 30.

weight, shoot dry weight, root length, fresh root weight, root dry weight, leaf area, leaf number, and leaf length. On the other hand, Arora et al. (2012) reported the positive effect of gold nanoparticles on various growth and yield-related parameters and suppressed pathogens.

The BioSeNPs in this study increased the content of photosynthetic pigments (chlorophyll and carotenoids). That may be because Bio-SeNPs surface surrounded with active phytochemicals in agreement with Hernández-Hernández et al. (2019), who stated that SeNPs increased the content of chlorophyll in tomato leaves. Also, El-Batal et al. (2016) found an increase in chlorophyll content in *Eruca sativa* treated with selenium nanoparticles. Furthermore, Dong et al. (2013) reported that selenium nanoparticles (10–50 ppm) significantly increased chlorogenic acid, chlorophyll and carotenoids by 200–400% of leaves of *Lycium chinense* L. Moreover, Ragavan et al. (2017), Vijayarengan (2013); and Sanghpriya Gautam (2015) reported that chemical selenium nanoparticles significantly increased the pigments in cluster beans.

On the same route, The improvement of gas exchange parameters by SeNPs application to wheat significantly reduces the plant's heat and drought stress and increases their yield (Djanaguiraman et al., 2018). High levels of stomata conductance are often required in the field to maximize cooling in the midday sun and to enhance photosynthetic yields (Roche, 2015). Consequently, the plant yield increased. There was a relationship between water stress and infection with *Fusarium* foot and root rot disease on durum wheat. The highest water stress level was more susceptible to disease severity caused by *F. culmorum* invading epidermal cells through stomata. Moreover, water stress level of 25% can affect 1000-grain weight, seedling stage and mature plants. The result indicates that the highest water stress treatment increased disease severity significantly when it subjected to 25% than 100% of water capacity (Chekali et al., 2011; Liu and Liu, 2016)

6. Conclusion

Bio-SeNPs can efficiently use against plant pathogenic fungi to protect wheat crop loss by CRDs, instead of using chemical nanoparticles and pesticides, which show higher toxicity to humans. Thus, it can say that Bio-SeNPs did not affect seed germination, root shoot ratio, and soil microflora, while some are beneficial to the plants. The nanoparticles are easily synthesized and subjugated as a fungicide foliar and fertilizer. Finally, it can conclude that Nanobiotechnology is an essential research area that deserves all our attention due to its potential application to agriculture.

Author contributions

M.T.E-S., A.M.S. and E.M.D. designed the study plan. E.S. and M. T.E-S., M. A. A. H helped in conducting the experiment and collected literature. S.E.E.F., A.A.N., S.O.A. and M.T.E.-S. analyzed the data and drafted the manuscript. S.E.E.F., A.A.N, S.O.A, F.M.A. and M.E.S. provided technical help in writing the manuscript. All the authors read and approved the final version of the manuscript.

Declaration of Competing Interest

No conflict of interests declared by the authors.

References

Ahmed, Z., Wang, Y., Anjum, N., Ahmad, A., Khan, S.T., 2013. Characterization of exopolysaccharide produced by *Lactobacillus kefiranofaciens* ZW3 isolated from Tibet kefir–Part II. Food Hydrocoll. 30 (1), 343–350.

Akl, B., Nader, M., El-Saadony, M.T., 2020. Biosynthesis of silver nanoparticles by *Serratia marcescens* ssp *sakuensis* and its antibacterial application against some pathogenic bacteria. J. Agric. Chem. Biotechnol. 11 (1), 1–8.

Alagesan, V., Venugopal, S., 2019. Green synthesis of selenium nanoparticle using leaves extract of *Withania somnifera* and its biological applications and photocatalytic activities. Bionanoscience 9 (1), 105–116.

Anyasi, T.A., Jideani, A.I.O., Mchau, G.R.A., 2017. Effects of organic acid pretreatment on microstructure, functional and thermal properties of unripe banana flour. J. Food Meas. Charact. 11 (1), 99–110.

Arora, S., Sharma, P., Kumar, S., Nayan, R., Khanna, P.K., Zaidi, M.G.H., 2012. Gold-nanoparticle induced enhancement in growth and seed yield of *Brassica juncea*. Plant Growth Regul. 66 (3), 303–310.

Bihari, P., Vippola, M., Schultes, S., Praetner, M., Khandoga, A.G., Reichel, C.A., Coester, C., Tuomi, T., Rehberg, M., Krombach, F., 2008. Optimized dispersion of nanoparticles for biological in vitro and in vivo studies. Part. Fibre Toxicol. 5 (1), 14. https://doi.org/10.1186/1743-8977-5-14.

Boroumand, S., Safari, M., Shaabani, E., Shirzad, M., Faridi-Majidi, R., 2019. Selenium nanoparticles: synthesis, characterization and study of their cytotoxicity, antioxidant and antibacterial activity. Mater. Res. Express 6 (8), 0850d8. https://doi.org/10.1088/2053-1591/ab2558.

Bunglavan, S.J., Garg, A.K., Dass, R.S., Shrivastava, S., 2014. Effect of supplementation of different levels of selenium as nanoparticles/sodium selenite on blood biochemical profile and humoral immunity in male Wistar rats. Vet. World 7 (12), 1075–1081.
Chekali, S., Gargouri, S., Paulitz, T., Nicol, J.M., Rezgui, M., Nasraoui, B., 2011. Effects of *Fusarium culmorum* and water stress on durum wheat in Tunisia. J. Crop Prot. 30 (6), 718–725.
Chen, T., Wong, Y.-S., Zheng, W., Bai, Y., Huang, L., 2008. Selenium nanoparticles fabricated in Undaria pinnatifida polysaccharide solutions induce mitochondria-mediated apoptosis in A375 human melanoma cells. Colloids Surf. B: Biointerfaces 67 (1), 26–31.
Dakal, T.C., Kumar, A., Majumdar, R.S., Yadav, V., 2016. Mechanistic basis of antimicrobial actions of silver nanoparticles. Front. Microbiol. 7, 1831.
Dhanjal, S., Cameotra, S., 2010. Aerobic biogenesis of selenium nanospheres by *Bacillus cereus* isolated from coalmine soil. Microb. Cell Factories 9 (1), 52. https://doi.org/10.1186/1475-2859-9-52.
Djanaguiraman, M., Boyle, D.L., Welti, R., Jagadish, S.V.K., Prasad, P.V.V., 2018. Decreased photosynthetic rate under high temperature in wheat is due to lipid desaturation, oxidation, acylation, and damage of organelles. BMC Plant Biol. 18 (1). https://doi.org/10.1186/s12870-018-1263-z.
Djanaguiraman, M., Devi, D.D., Shanker, A.K., Sheeba, J.A., Bangarusamy, U., 2005. Selenium–an antioxidative protectant in soybean during senescence. Plant and Soil 272 (1-2), 77–86.
Dong, J.Z., Wang, Y., Wang, S.H., Yin, L.P., Xu, G.J., Zheng, C., Lei, C., Zhang, M.Z., 2013. Selenium increases chlorogenic acid, chlorophyll and carotenoids of *Lycium chinense* leaves. J. Sci. Food Agric. 93 (2), 310–315.
Dorofeev, G., Streletskii, A., Povstugar, I., Protasov, A., Elsukov, E., 2012. Determination of nanoparticle sizes by X-ray diffraction. Colloid J. 74, 675–685.
Drake, P.L., Froend, R.H., Franks, P.J., 2013. Smaller, faster stomata: scaling of stomatal size, rate of response, and stomatal conductance. J. Exp. Bot. 64, 495–505.
El-Batal, A.I., Sidkey, N.M., Ismail, A., Arafa, R.A., Fathy, R.M., 2016. Impact of silver and selenium nanoparticles synthesized by gamma irradiation and their physiological response on early blight disease of potato. J. Chem. Pharm. Res 8, 934–951.
El-Saadony, M.T., El-Wafai, N., El-Fattah, H., Mahgoub, S., 2019. Biosynthesis, optimization and characterization of silver nanoparticles using a soil isolate of *Bacillus pseudomycoides* MT32 and their antifungal activity against some pathogenic fungi. Adv. Anim. Vet. Sci 7, 238–249.
El-Saadony, M.T., El-Hack, A., Mohamed, E., Taha, A.E., Fouda, M.M., Ajarem, J.S., N Maodaa, S., Allam, A.A., Elshaer, N.J.N., 2020a. Ecofriendly synthesis and insecticidal application of copper nanoparticles against the storage pest Tribolium castaneum. Nanomaterials, 10, 587.
El-Saadony, M.T., El-Wafai, N.A., El-Fattah, A., Mahgoub, S., 2018. Biosynthesis, optimization and characterization of silver nanoparticles biosynthesized by *Bacillus subtilis* ssp *spizizenii* MT5 isolated from heavy metals polluted soil. Zagazig J. Agric. Res. 45, 2439–2454.
El-Saadony, M.T., Elsadek, M.F., Mohamed, A.S., Taha, A.E., Ahmed, B.M., Saad, A.M., 2020b. Effects of chemical and natural additives on cucumber juice's quality, shelf life, and safety. Foods 9, 639.
El-Saadony, M.T., Desoky, E.S.M., Saad, A.M., Eid, R.S., Selem, E., Elrys, A.S., 2021a. Biological silicon nanoparticles improve *Phaseolus vulgaris* L. yield and minimize its contaminant contents on a heavy metals-contaminated saline soil. J. Environ. Sci. 106, 1–14.
El-Saadony, M.T., Sitohy, M.Z., Ramadan, M.F., Saad, A.M., 2021b. Green nanotechnology for preserving and enriching yogurt with biologically available iron (II). Innov. Food Sci. Emerg. Technol. 69, (1) 102645.
FAO, 2015. http://agrinvestment.egyptagriculture.net/EN/mediacenter/publications/17/77/.
FAO, 2018. Http: //www.fao.org/giews/countrybrief/country.jspcode=EGY.
Fesharaki, P.J., Nazari, P., Shakibaie, M., Rezaie, S., Banoee, M., Abdollahi, M., Shahverdi, A.R., 2010. Biosynthesis of selenium nanoparticles using *Klebsiella pneumoniae* and their recovery by a simple sterilization process. Braz. J. Microbiol. 41, 461–466.
Germ, M., Kreft, I., Osvald, J., 2005. Influence of UV-B exclusion and selenium treatment on photochemical efficiency of photosystem II, yield and respiratory potential in pumpkins (*Cucurbita pepo* L.). Plant Physiol. Biochem. 43, 445–448.
Gil, M.I., Tomás-Barberán, F.A., Hess-Pierce, B., Kader, A.A., 2002. Antioxidant capacities, phenolic compounds, carotenoids, and vitamin C contents of nectarine, peach, and plum cultivars from California. J. Agric. Food Chem. 50, 4976–4982.
Gunti, L., Dass, R.S., Kalagatur, N.K., 2019. Phytofabrication of selenium nanoparticles from *Emblica officinalis* fruit extract and exploring its biopotential applications: antioxidant, antimicrobial, and biocompatibility. Front. Microbiol. 10, 931.
Hariharan, H., Al-Harbi, N., Karuppiah, P., Rajaram, S., 2012. Microbial synthesis of selenium nanocomposite using *Saccharomyces cerevisiae* and its antimicrobial activity against pathogens causing nosocomial infection. Chalcogenide Lett. 9, 509–515.
Hartikainen, H., Xue, T., Piironen, V., 2000. Selenium as an anti-oxidant and pro-oxidant in ryegrass. Plant and soil 225, 193–200.
Hernández-Hernández, H., Quiterio-Gutiérrez, T., Cadenas-Pliego, G., Ortega-Ortiz, H., Hernández-Fuentes, A.D., Cabrera de la Fuente, M., Valdés-Reyna, J., Juárez-Maldonado, A., 2019. Impact of selenium and copper nanoparticles on yield, antioxidant system, and fruit quality of tomato plants. Plants 8, 355.
Hnain, A., Brooks, J., Lefebvre, D.D., 2013. The synthesis of elemental selenium particles by *Synechococcus leopoliensis*. Appl. Microbiol. Biotechnol. 97, 10511–10519.
Hu, C., Li, Y., Xiong, L., Zhang, H., Song, J., Xia, M., 2012. Comparative effects of nano elemental selenium and sodium selenite on selenium retention in broiler chickens. Anim. Feed Sci. Technol. 177, 204–210.
Huang, Z., Guo, B., Wong, R., Jiang, Y., 2007. Characterization and antioxidant activity of selenium-containing phycocyanin isolated from *Spirulina platensis*. Food Chem. 100, 1137–1143.
Ikram, M., Raja, N.I., Javed, B., Hussain, M., Hussain, M., Ehsan, M., Rafique, N., Malik, K., Sultana, T., Akram, A., 2020. Foliar applications of bio-fabricated selenium nanoparticles to improve the growth of wheat plants under drought stress. Green Process Synth. 9, 706–714.
Ingole, A.R., Thakare, S.R., Khati, N., Wankhade, A.V., Burghate, D., 2010. Green synthesis of selenium nanoparticles under ambient condition. Chalcogenide Lett. 7, 485–489.
Ismail, A.-W.A., Sidkey, N.M., Arafa, R.A., Fathy, R.M., El-Batal, A.I., 2016. Evaluation of in vitro antifungal activity of silver and selenium nanoparticles against *Alternaria solani* caused early blight disease on potato. British Biotechnol. J. 12 (3), 1–11.
Janga, M.R., Raoof, M., Ulaganathan, K., 2017. Effective biocontrol of Fusarium wilt in castor (*Ricinius communis* L.) with *Bacillus* sp. in pot experiments. Rhizosphere 3, 50–52.
Jo, Y.-K., Kim, B.H., Jung, G., 2009. Antifungal activity of silver ions and nanoparticles on phytopathogenic fungi. Plant Dis. 93, 1037–1043.
Kalagatur, N.K., Kamasani, J.R., Mudili, V., 2018. Assessment of detoxification efficacy of irradiation on zearalenone mycotoxin in various fruit juices by response surface methodology and elucidation of its in-vitro toxicity. Front. microbiol. 9, 2937.
Kalagatur, N.K., Mudili, V., Siddaiah, C., Gupta, V.K., Natarajan, G., Sreepathi, M.H., Vardhan, B.H., Putcha, V.L., 2015. Antagonistic activity of *Ocimum sanctum* L. essential oil on growth and zearalenone production by *Fusarium graminearum* in maize grains. Front. Microbiol. 6, 892.
Kapur, M., Soni, K., Kohli, K., 2017. Green synthesis of selenium nanoparticles from broccoli, characterization, application and toxicity. Adv. Tech. Biol. Med. 5 (2379–1764), 1000198.
Karaduman, A., Ozaslan, M., H Kilic, I., Bayil-Oguzkan, S., Kurt, B.S., Erdogan, N., 2017. Identification by using MALDI-TOF mass spectrometry of lactic acid bacteria isolated from non-commercial yogurts in southern Anatolia, Turkey. Int. Microbiol. 20, 25-30.
Kaur, P.T., R.; Chaudhary, A. , 2011. Biosynthesis of silver nanoparticles using flower extract of Calendula officinalis Plant. Adv. Conv. technolo. 109-113.
Kazempour, Z.B., Yazdi, M.H., Rafii, F., Shahverdi, A.R., 2013. Sub-inhibitory concentration of biogenic selenium nanoparticles lacks post antifungal effect for *Aspergillus niger* and *Candida albicans* and stimulates the growth of *Aspergillus niger*. Iranian J. Microbiol. 5, 81.
Khaledi, N., Taheri, P., Falahati-Rastegar, M., 2018. Evaluation of resistance and the role of some defense responses in wheat cultivars to *Fusarium* head blight. J. Plant Prot. Res. 57 (4), 398–408.
Lamsa, K., Kim, S.-W., Jung, J.H., Kim, Y.S., Kim, K.S., Lee, Y.S., 2011. Inhibition effects of silver nanoparticles against powdery mildews on cucumber and pumpkin. Mycobiology 39, 26–32.
Liu, X., Liu, C., 2016. Effects of Drought-Stress on *Fusarium* Crown Rot Development in Barley. PloS one 11.
Lyons, G.H., Genc, Y., Soole, K., Stangoulis, J., Liu, F., Graham, R., 2009. Selenium increases seed production in Brassica. Plant and Soil 318, 73–80.
Ma, L., Ji, Z., Bao, J., Zhu, X., Li, X., Zhuang, J., Yang, C., Xia, Y., 2008. Responses of rice genotypes carrying different dwarf genes to *Fusarium moniliforme* and gibberellic acid. Plant Prod. Sci. 11, 134–138.
Moya-Elizondo, E.A., Jacobsen, B.J., 2016. Integrated management of *Fusarium* crown rot of wheat using fungicide seed treatment, cultivar resistance, and induction of systemic acquired resistance (SAR). Biol. Control 92, 153–163.
Nagata, M., Yamashita, I., 1992. Simple method for simultaneous determination of chlorophyll and carotenoids in tomato fruit. Nippon Shokuhin Kogyo Gakkaishi 39, 925–928.
Nandini, B., Hariprasad, P., Prakash, H.S., Shetty, H.S., Geetha, N., 2017. Trichogenic-selenium nanoparticles enhance disease suppressive ability of *Trichoderma* against downy mildew disease caused by *Sclerospora graminicola* in pearl millet. Sci. Rep. 7, 1–11.
Ocsoy, I., Paret, M.L., Ocsoy, M.A., Kunwar, S., Chen, T., You, M., Tan, W., 2013. Nanotechnology in plant disease management: DNA-directed silver nanoparticles on graphene oxide as an antibacterial against *Xanthomonas perforans*. Acs Nano. 7, 8972–8980.
Parsons, M., Munkvold, G., 2012. Effects of planting date and environmental factors on *Fusarium* ear rot symptoms and fumonisin B1 accumulation in maize grown in six North American locations. Plant Pathol. 61, 1130–1142.
Pierard, G., Arrese, J., Piérard-Franchimont, C., De Doncker, P., 1997. Prolonged effects of antidandruff shampoos-time to recurrence of *Malassezia ovalis* colonization of skin. Int. J. Cosmet. Sci. 19, 111–117.
Ragavan, P., Ananth, A., Rajan, M., 2017. Impact of selenium nanoparticles on growth, biochemical characteristics and yield of cluster bean *Cyamopsis tetragonoloba*. Int. J. Environ. Agric. Biotechnol. 2, 238983.
Rajasree, R.S., 2015. Extracellular biosynthesis of selenium nanoparticles using some species of *lactobacillus*. Indian J. Mar. Sci. 43 (5), 766–775.
Reda, F.M., El-Saadony, M.T., Elnesr, S.S., Alagawany, M., Tufarelli, V., 2020. Effect of dietary supplementation of biological curcumin nanoparticles on growth and

carcass traits, antioxidant status, immunity and caecal microbiota of Japanese quails. Animals 10, 754.
Reda, F.M., El-Saadony, M.T., El-Rayes, T.K., Attia, A.I., El-Sayed, S.A., Ahmed, S.Y., Alagawany, M., 2021. Use of biological nano zinc as a feed additive in quail nutrition: biosynthesis, antimicrobial activity and its effect on growth, feed utilisation, blood metabolites and intestinal microbiota. Ital. J. Anim. Sci. 20 (1), 324–335.
Rocha, O., Ansari, K., Doohan, F.M., 2005. Effects of trichothecene mycotoxins on eukaryotic cells: a review. Food Addit Contam. 22, 369–378.
Roche, D., 2015. Stomatal conductance is essential for higher yield potential of C3 crops. Crit. Rev. Plant Sci. 34, 429–453.
Salaj, R., Štofilová, J., Šoltesová, A., Hertelyová, Z., Hijová, E., Bertková, I., Strojný, L., Kružliak, P., Bomba, A., 2013. The effects of two *Lactobacillus plantarum* strains on rat lipid metabolism receiving a high fat diet. Sci. World J. 2013, (8) 135142.
Sanghpriya Gautam, P.K.S.M.N., 2015. Growth and biochemical responses of spinach (*Spinacea oleracea* L.) grown in Zn contaminated soils. Int. J. Recent Biotechnol. 3, 7–12.
Sasidharan, S., Sowmiya, R., Balakrishnaraja, R., 2014. Biosynthesis of selenium nanoparticles using citrus reticulata peel extract. World J. Pharm. Res 4, 1322–1330.
Shah, L., Ali, A., Yahya, M., Zhu, Y., Wang, S., Si, H., Rahman, H., Ma, C., 2018. Integrated control of fusarium head blight and deoxynivalenol mycotoxin in wheat. Plant Pathol. 67, 532–548.
Shah, V., Belozerova, I., 2009. Influence of metal nanoparticles on the soil microbial community and germination of lettuce seeds. Water Air Soil Pollut. 197, 143–148.
Shahverdi, A., Fakhimi, A., Mosavat, G., Jafari-Fesharaki, P., Rezaie, S., Rezayat, S., 2010. Antifungal activity of biogenic selenium nanoparticles. World Appl. Sci. J. 10, 918–922.
Sheiha, A.M., Abdelnour, S.A., El-Hack, A., Mohamed, E., Khafaga, A.F., Metwally, K.A., Ajarem, J.S., Maodaa, S.N., Allam, A.A., El-Saadony, M.T., 2020. Effects of dietary biological or chemical-synthesized nano-selenium supplementation on growing rabbits exposed to thermal stress. Animals 10, 430.
Shenashen, M., Derbalah, A., Hamza, A., Mohamed, A., El Safty, S., 2017. Antifungal activity of fabricated mesoporous alumina nanoparticles against root rot disease of tomato caused by *Fusarium oxysporium*. Pest Manag. Sci. 73, 1121–1126.
Shewry, P.R., Hey, S.J., 2015. The contribution of wheat to human diet and health. Food Energy Secur. 4, 178–202.
Shubharani, R., Mahesh, M., Yogananda Murth V. N, 2019. Biosynthesis and characterization, antioxidant and antimicrobial activities of selenium nanoparticles from ethanol extract of Bee Propolis. J. Nanomed. Nanotechnol. 2019, 10(01).
Srivastava, N., Mukhopadhyay, M., 2013. Biosynthesis and structural characterization of selenium nanoparticles mediated by *Zooglea ramigera*. Powder Technol. 244, 26–29.
Srivastava, N., Mukhopadhyay, M., 2015. Biosynthesis and structural characterization of selenium nanoparticles using *Gliocladium roseum*. J. Clust. Sci. 26, 1473–1482.
Uddin, Q., Samiulla, L., Singh, V.K., Jamil, S.S., 2012. Phytochemical and pharmacological profile of Withania somnifera dunal: A review. J. Appl. Pharm. Sci. 2, 170–175.
Vieira, E.F., Carvalho, J., Pinto, E., Cunha, S., Almeida, A.A., Ferreira, I.M., 2016. Nutritive value, antioxidant activity and phenolic compounds profile of brewer's spent yeast extract. J. Food Compos. Anal. 52, 44–51.
Vijayarengan, P., 2013. Changes in growth, biochemical constituents and antioxidant potentials in cluster bean *Cyamopsis tetragonoloba* L. Taub under zinc stress. Int. J. Curr. Sci. 5, 37–49.
Vyas, J., Rana, S., 2017. Antioxidant activity and green synthesis of selenium nanoparticles using *allium sativum* extract. Int. J. Phytomedicine 9, 634.
Wegulo, N. Stephen, Baenziger, P. Stephen, Nopsa, J Hernandez, Bockus, William W., Hallen-Adams, Heather, 2015. Management of Fusarium head blight of wheat and barley.. Crop Protection 73, 100–107.
Xu, B.J., Chang, S., 2007. A comparative study on phenolic profiles and antioxidant activities of legumes as affected by extraction solvents. J. food Sci. 72, S159–S166.
Xue, A.G., Guo, W., Chen, Y., Siddiqui, I., Marchand, G., Liu, J., Ren, C., 2017. Effect of seed treatment with novel strains of *Trichoderma* spp. on establishment and yield of spring wheat. Crop Prot. 96, 97–102.
Zakharova, O.V., Gusev, A.A., Zherebin, P.M., Skripnikova, E.V., Skripnikova, M.K., Ryzhikh, V.E., Lisichkin, G.V., Shapoval, O.A., Bukovskii, M.E., Krutyakov, Y.A., 2017. Sodium tallow amphopolycarboxyglycinate-stabilized silver nanoparticles suppress early and late blight of Solanum lycopersicum and stimulate the growth of tomato plants. BioNanoScience 7, 692–702.
Zhai, X., Zhang, C., Zhao, G., Stoll, S., Ren, F., Leng, X., 2017. Antioxidant capacities of the selenium nanoparticles stabilized by chitosan. J. Nanobiotechnol. 15, 1–12.
Zhang, W., Chen, Z., Liu, H., Zhang, L., Gao, P., Li, D., 2011. Biosynthesis and structural characteristics of selenium nanoparticles by *Pseudomonas alcaliphila*. Colloids Surf. B: Biointerfaces 88, 196–201.